Molecular Mimicry-Based Repositioning of Nutlin-3 to Anti-Apoptotic Bcl-2 Family Proteins

Ji-Hyang Ha,[†] Eun-Young Won,[†] Jae-Sun Shin,[†] Mi Jang,[†] Kyoung-Seok Ryu,[‡] Kwang-Hee Bae,[†] Sung Goo Park,[†] Byoung Chul Park,[†] Ho Sup Yoon,*,[§] and Seung-Wook Chi*,[†]

[†]Medical Proteomics Research Center, KRIBB, Daejeon 305-806, Republic of Korea

[‡]Division of Magnetic Resonance, Korea Basic Science Institute Ochang Campus, Cheongwon-Gun, Ochang-Eup, Yangcheong-Ri 804-1, Chungcheongbuk-Do 363-883, Republic of Korea

[§]Division of Structural and Computational Biology, School of Biological Sciences, Nanyang Technological University, 60 Nanyang Drive, Singapore 637511, Singapore

Ⓢ *Supporting Information*

ABSTRACT: The identification of off-target binding of drugs is a key to repositioning drugs to new therapeutic categories. Here we show the universal interactions of the p53 transactivation domain (p53TAD) with various anti-apoptotic Bcl-2 family proteins via a mouse double minute 2 (MDM2) binding motif, which play an important role in transcription-independent apoptotic pathways of p53. Interestingly, our structural studies reveal that the anti-apoptotic Bcl-2 family proteins and MDM2 share a similar mode of interaction with the p53TAD. On the basis of this close molecular mimicry, our NMR results demonstrate that the potent MDM2 antagonists Nutlin-3 and PMI bind to the anti-apoptotic Bcl-2 family proteins in a manner analogous to that with the p53TAD.

Drug repositioning has been an emerging strategy in drug discovery, as an understanding of novel uses for existing drugs could provide insightful information into the molecular mechanisms and safety of drugs.[1] Although unexpected off-target binding of drugs usually induces unwanted and harmful side effects, such binding can sometimes be useful for repositioning drugs to new therapeutic categories. A variety of off-target bindings observed in marketed drugs suggest a broad spectrum of physiological targets.[2] Thus, it is necessary to identify additional hidden targets of existing drugs and drug candidates for their potential use in different therapeutic indications.

Blocking the p53—mouse double minute 2 (MDM2) interaction has been an attractive strategy for anticancer therapy. In particular, the α-helical motif present in the p53 transactivation domain (p53TAD) (residues Ser15—Asn29, herein termed SN15) complexed with MDM2[3] has served as a useful structural template for designing novel MDM2 inhibitors as anticancer therapeutic agents. As the structure of Nutlin mimics that of the SN15 peptide bound to MDM2, it serves as a competitive inhibitor of the p53—MDM2 interaction.[4,5] Currently, Nutlins are being evaluated as cancer therapeutics in clinical trials.

The Bcl-2 family proteins are critical regulators of apoptosis, as they control the permeability of the outer mitochondrial membrane and the release of cytochrome c.[6−8] In response to apoptotic stimuli, p53 rapidly translocates to the mitochondria and interacts with anti-apoptotic Bcl-2 family proteins at the mitochondria, inducing transcription-independent apoptosis of p53.[8] To provide insights into how the p53 N-terminal domain (p53NTD) alone, without the p53 DNA-binding domain (p53DBD), is able to induce apoptosis in the absence of transcriptional activity,[9,10] we demonstrated that the MDM2-binding SN15 motif in the p53TAD also acts as a Bcl-X_L binding motif.[11,12]

Is the above-mentioned interaction specific to Bcl-X_L or common to the Bcl-2 family proteins? As the anti-apoptotic Bcl-2 family proteins exhibit nearly identical three-dimensional structural folds, we hypothesized that other Bcl-2 family proteins might interact with p53 in a manner similar to that seen in Bcl-X_L. We tested this hypothesis by carrying out glutathione S-transferase (GST) pull-down experiments in BOSC 23 (human embryonic kidney cell line) cells. Both the GST-tagged p53NTD and p53TAD were pulled down with FLAG-tagged Bcl-2, Bcl-w, Mcl-1, and Kaposi sarcoma-associated herpes virus (KSHV) Bcl-2, indicating the molecular interaction between the p53TAD and the Bcl-2 family proteins (Figure S1 in the Supporting Information). The results prompted us to further define the Bcl-2 family protein-binding site on the p53TAD. To this end, we monitored the chemical shift perturbation of the ^{15}N-labeled p53TAD in the presence of Bcl-2, Bcl-w, and Mcl-1 using NMR spectroscopy (Figure S2). During titration, notable line broadening and chemical shift perturbations on the cross-peaks of p53TAD residues 16—30 and 40—56 were observed upon the addition of the anti-apoptotic Bcl-2 family proteins (Figure 1a). Notably, these chemical shift perturbation patterns of the p53TAD are quite similar to those observed in binding of MDM2, indicating that the p53TAD interacts with all of the anti-apoptotic Bcl-2 family members tested via the same MDM2-binding motif. On the other hand, chemical shift perturbations of the ^{15}N-labeled Bcl-2 family proteins Bcl-2, Bcl-w, Mcl-1, and KSHV Bcl-2 in the presence of the SN15 peptide (Figure 1b and Figure S3) showed that the p53TAD binds to the pro-apoptotic BH3 peptide-binding hydrophobic grooves of the anti-apoptotic Bcl-2 family proteins surrounded by the BH1, BH2, and BH3 regions. Taken together, our results suggest that the p53TAD—Bcl-2 family interaction might be a universally conserved molecular
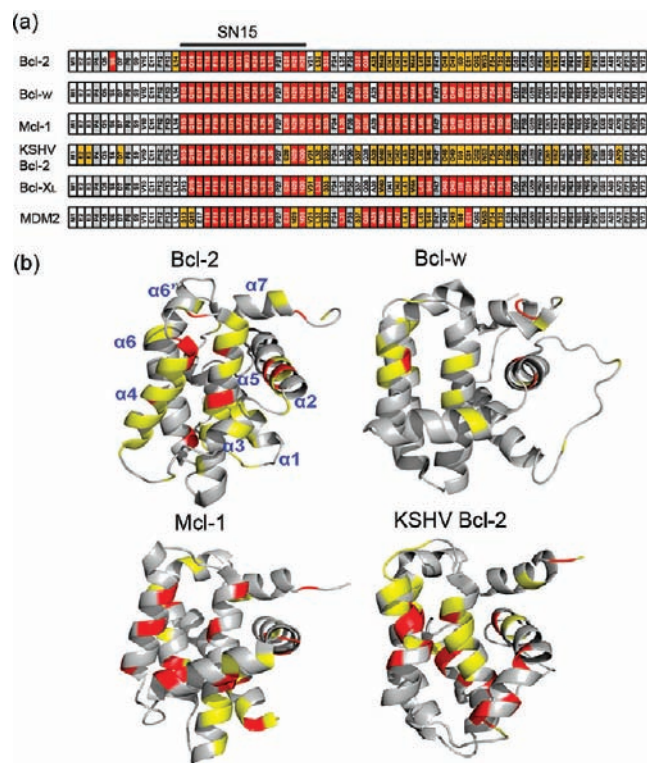
Figure 1. Binding site mapping of the interaction between the p53TAD and anti-apoptotic Bcl-2 family proteins. (a) Sequence-based chemical shift perturbation maps of the p53TAD upon binding to Bcl-2 family proteins and MDM2. The red-colored region indicates cross-peaks of the p53TAD that disappeared or were weakened upon binding, whereas the orange-colored region shows cross-peaks that moved. The cross-peaks that remained unaffected by binding and prolines are shown in white and gray, respectively. (b) SN15 peptide-binding site mapped on Bcl-2 family proteins. The residues showing chemical shift changes with $\Delta CS > 0.08$ and $0.03 < \Delta CS < 0.08$ are colored red and yellow, respectively.

Figure 2. Structural model for the Bcl-2/SN15 peptide complex. (a) Structural models of the Bcl-2/SN15 and Bcl-X_L/SN15 complexes compared with the crystal structure of the Bcl-X_L/Bak complex. The SN15 and Bak peptides are shown in yellow and red, respectively. (b) Chemical shift perturbations of Bcl-2 residues upon binding to the alanine mutants of SN15. Resonances that disappeared upon binding are shown as gray bars.

mechanism for regulation of anti-apoptotic Bcl-2 family proteins by p53.

To orient the SN15 peptide in the binding site of Bcl-2, we performed paramagnetic relaxation enhancement (PRE) NMR experiments. The two-dimensional (2D) ^{1}H$-^{15}$N heteronuclear single-quantum coherence (HSQC) spectra of ^{15}N-labeled Bcl-2 were acquired in the presence of methane thiosulfonate (MTSL)-derivatized Cys-SN15 peptide in the oxidized and reduced states (Figure S4). A specific paramagnetic broadening effect on the cross-peaks of the Bcl-2 residues that mainly reside in the α2 and α5 helices (e.g., Phe104, Trp144, Gly145, Ile147, Val148, Glu152, and Gly154) was clearly observed. Our results indicate that the N-terminus of the SN15 peptide is oriented toward the α2 and α5 helices of Bcl-2. Thus, the orientations of the SN15 and Bak BH3 peptides in the binding site of Bcl-2/Bcl-X_L are opposite, although they occupy the same binding site in Bcl-2 and Bcl-X_L.

On the basis of the chemical shift perturbations and the PRE data, we present a structural model for complexes of the p53TAD and anti-apoptotic Bcl-2 family proteins (Figure 2a). Our structural models of the Bcl-2/SN15 and Bcl-X_L/SN15 complexes reveal a highly conserved binding mechanism of the p53TAD with anti-apoptotic Bcl-2 family proteins. To validate our structural model, we conducted NMR binding experiments of Bcl-2
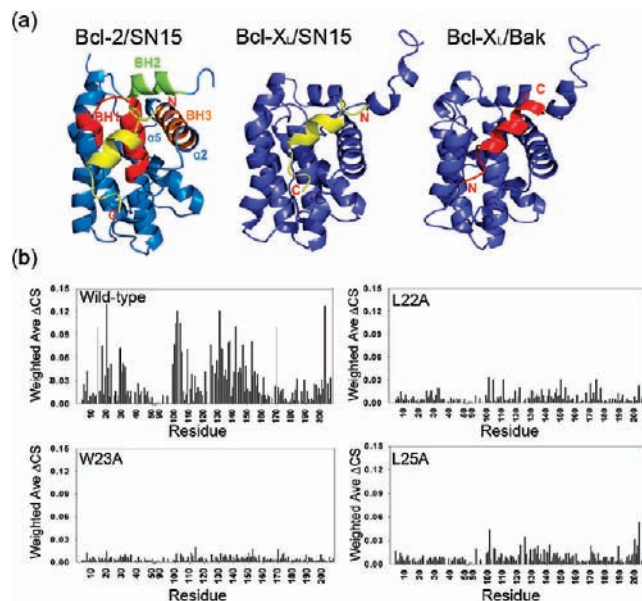
with mutant SN15 peptides having an alanine replacement at the respective position of residues 18−26. The alanine substitutions at Leu22, Trp23, and Leu25 completely abolished the NMR chemical shift perturbation (Figure 2b). In addition, alanine substitutions at Phe19, Lys24, and Leu26 substantially diminished the chemical shift perturbations seen in the presence of the wild-type SN15 peptide. Consistent with the structural model, the mutagenesis data showed that these hydrophobic residues in the SN15 peptide are key binding determinants for Bcl-2 and that they coincide with those crucial for interaction with MDM2.[13]

Interestingly, structural comparison of the Bcl-2/SN15 and Bcl-X_L/SN15 complexes with the previously determined MDM2/SN15[3] and p300 Taz2/p53 (2−39)[14] complexes revealed that they share a similar mode of interaction despite the difference in their global folds. The hydrophobic residues aligned on one face of the amphipathic SN15 α-helix are commonly involved in the interactions with the binding partner (Figure 3). However, there is a noticeable difference in the key binding determinants, depending on the binding partner. In the Bcl-2/Bcl-X_L and MDM2 complexes, Phe19, Leu22, Trp23, and Leu26 of the SN15 peptide form key hydrophobic interactions, and the aromatic ring of Trp23 fits snugly into the binding pocket, making the largest contribution to stabilizion of the complexes. On the other hand, Phe19, Leu22, and Leu25 of the SN15 peptide participate in key interactions in the p300 Taz2 complex, in which Trp23 and Leu26 project away from the p300 Taz2 molecule (Figure 3d). Thus, the way the p53TAD interacts with the anti-apoptotic Bcl-2 family proteins is quite similar to what is shown in the interaction between p53TAD and MDM2.

On the basis of the close mimicry in recognition of the Bcl-2 family proteins and MDM2 by the p53TAD, we postulated that like the SN15 peptide, SN15-mimetic MDM2 antagonists can bind to anti-apoptotic Bcl-2 family proteins. We tested this
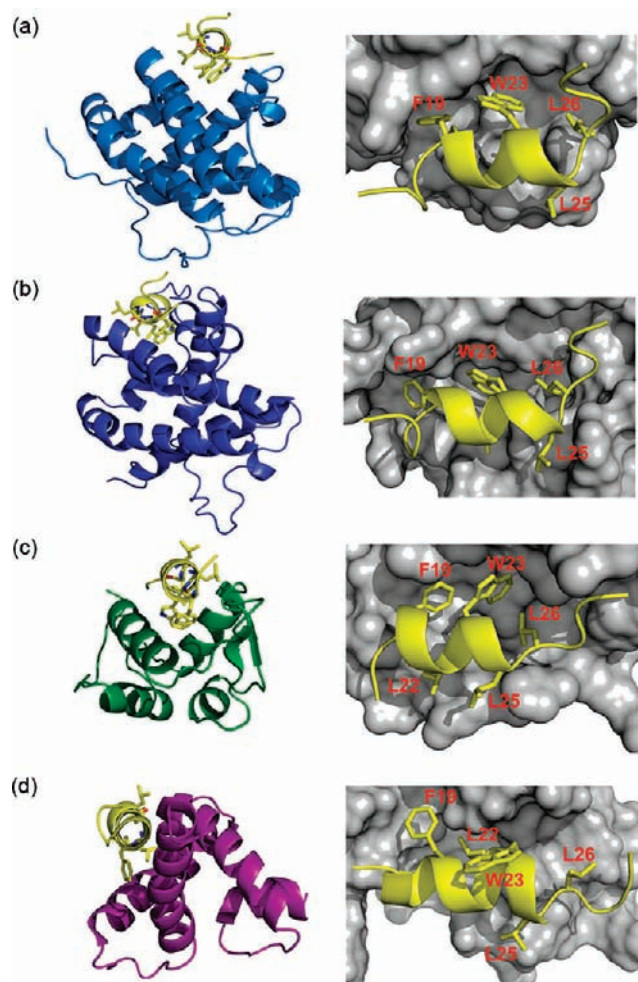
Figure 3. Mimicry in the recognition of anti-apoptotic Bcl-2 family proteins and MDM2 by the p53TAD. Structural models of the (a) Bcl-2/SN15 and (b) Bcl-X_L/SN15 complexes were compared with the previously reported structures of the (c) MDM2/SN15 and (d) p300 Taz2/SN15 complexes. The SN15 peptides are drawn as yellow ribbon models, and the residues involved in binding are labeled.

Figure 4. Binding of Nutlin-3 and PMI to anti-apoptotic Bcl-X_L. (a, b) Overlaid 2D $^{1}H-^{15}N$ HSQC spectra for ^{15}N-labeled Bcl-X_L in the absence (blue) and presence (red) of (a) Nutlin-3 and (b) PMI. (c) Chemical shift perturbations of Bcl-X_L upon binding to Nutlin-3. Resonances that disappeared upon binding are shown as gray bars. (d) Plots of chemical shift changes in Bcl-X_L resonances induced by Nutlin-3. (e) Displacement of ^{15}N-labeled p53TAD from Bcl-X_L by the addition of Nutlin-3 (red). The blue cross-peaks represent NMR resonances for free ^{15}N-labeled p53TAD, and the green cross-peaks represent those for ^{15}N-labeled p53TAD bound to Bcl-X_L. (f) Chemical shift perturbations of Bcl-X_L induced by Nutlin-3 mapped onto the structure of Bcl-X_L complexed with ABT-737. The Bcl-X_L residues showing chemical shift changes of $\Delta CS > 0.2$ are colored yellow, and residues for which the cross-peaks disappeared upon binding of Nutlin-3 are colored red.

hypothesis through NMR titration experiments of the ^{15}N-labeled Bcl-2 family proteins Bcl-X_L and Bcl-2 with Nutlin-3 and PMI, a potent MDM2 inhibitor selected from a phage-displayed peptide library[15] (Figure 4a,b and Figure S5). When Bcl-X_L was bound to Nutlin-3 or PMI, the cross-peaks from the BH1, BH2, and BH3 regions of Bcl-X_L moved to a large extent (Figure 4c). For the binding of Nutlin-3 to Bcl-X_L, a K_D value of 15 μM was determined by fitting the NMR chemical shift perturbation data to a single-site ligand binding model (Figure 4d). The residues of Bcl-2 and Bcl-X_L perturbed by binding to Nutlin-3 were almost the same as those perturbed by binding to the SN15 peptide, suggesting that Nutlin-3 directly binds to both Bcl-2 and Bcl-X_L in a manner analogous to that with the SN15 peptide. We confirmed this by performing a 2D $^{1}H-^{15}N$ HSQC NMR competition experiment in which the ^{15}N-labeled p53TAD/Bcl-X_L complex was titrated with Nutlin-3. When increasing amounts of Nutlin-3 were added, the NMR signals of the SN15 motif that had disappeared upon binding (e.g., those from Phe19, Leu22, Trp23, Leu25, and Leu26) were recovered at the position of free p53TAD (Figure 4e). This result indicates that Nutlin-3 and the SN15 motif compete directly for
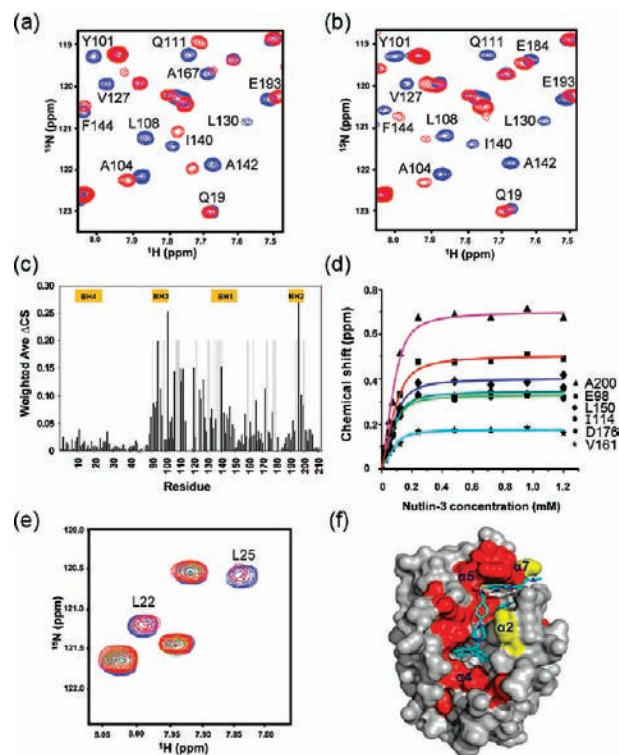
the same binding site in Bcl-X_L. Analysis of mapping of the Nutlin-3-induced chemical shift perturbations onto the Bcl-X_L structure suggested that the binding of Nutlin-3 occurs at the binding site for the Bcl-2/Bcl-X_L inhibitor ABT-737[16] (Figure 4f).

In this study, we have uncovered off-target binding of the MDM2 antagonist Nutlin-3 to the anti-apoptotic Bcl-2 family proteins Bcl-X_L and Bcl-2. Our findings may provide insights into the molecular basis of how transcription-independent mitochondrial apoptosis of p53 makes a major contribution to Nutlin-induced apoptosis in tumor cells.[17,18] On the basis of the dual role of the p53TAD in apoptosis in different cellular compartments, we suggest a molecular mechanism of the dual target-based apoptosis of Nutlin in cancer cells (Figure S6): (1) Nutlin binds to MDM2, releasing p53 from the p53/MDM2 complex and triggering apoptosis via the transcriptional activity of p53; (2) at the mitochondria, Nutlin directly binds to anti-apoptotic Bcl-X_L and Bcl-2, liberating pro-apoptotic Bak/Bax from complexes and eventually inducing apoptosis in a transcription-independent manner. Concomitant inhibition of MDM2 and Bcl-2 function displayed a synergistic apoptotic effect in cancers

such as acute myeloid leukemia (AML).[19] Thus, a novel dual target-based therapeutic strategy may have important implications for the clinical use of Nutlin-like compounds.

In summary, we have reported the universal interactions of the p53TAD with various anti-apoptotic Bcl-2 family proteins, which play an important role in transcription-independent apoptosis mechanism of p53. From the NMR studies, we have provided "proof-of-concept" evidence that the potent MDM2 antagonists Nutlin-3 and PMI directly bind to anti-apoptotic Bcl-2 family proteins and proposed a novel dual target-based therapeutic strategy for Nutlin.

■ ASSOCIATED CONTENT

Ⓢ Supporting Information. Experimental procedures, Figures S1–S6, and complete ref 16. This material is available free of charge via the Internet at http://pubs.acs.org.

■ AUTHOR INFORMATION

Corresponding Author
swchi@kribb.re.kr; hsyoon@ntu.edu.sg

■ ACKNOWLEDGMENT

■ REFERENCES

(1) Ashburn, T. T.; Thor, K. B. *Nat. Rev. Drug Discovery* **2004,** *3,* 673.

(2) Campillos, M.; Kuhn, M.; Gavin, A. C.; Jensen, L. J.; Bork, P. *Science* **2008,** *321,* 263.

(3) Kussie, P. H.; Gorina, S.; Marechal, V.; Elenbaas, B.; Moreau, J.; Levine, A. J.; Pavletich, N. P. *Science* **1996,** *274,* 948.

(4) Vassilev, L. T.; Vu, B. T.; Graves, B.; Carvajal, D.; Podlaski, F.; Filipovic, Z.; Kong, N.; Kammlott, U.; Lukacs, C.; Klein, C.; Fotouhi, N.; Liu, E. A. *Science* **2004,** *303,* 844.

(5) Fesik, S. W. *Nat. Rev. Cancer* **2005,** *5,* 876.

(6) Chipuk, J. E.; Kuwana, T.; Bouchier-Hayes, L.; Droin, N. M.; Newmeyer, D. D.; Schuler, M.; Green, D. R. *Science* **2004,** *303,* 1010.

(7) Leu, J. I.; Dumont, P.; Hafey, M.; Murphy, M. E.; George, D. L. *Nat. Cell Biol.* **2004,** *6,* 443.

(8) Mihara, M.; Erster, S.; Zaika, A.; Petrenko, O.; Chittenden, T.; Pancoska, P.; Moll, U. M. *Mol. Cell* **2003,** *11,* 577.

(9) Chipuk, J. E.; Maurer, U.; Green, D. R.; Schuler, M. *Cancer Cell* **2003,** *4,* 371.

(10) Sayan, B. S.; Sayan, A. E.; Knight, R. A.; Melino, G.; Cohen, G. M. *J. Biol. Chem.* **2006,** *281,* 13566.

(11) Xu, H.; Tai, J.; Ye, H.; Kang, C. B.; Yoon, H. S. *Biochem. Biophys. Res. Commun.* **2006,** *341,* 938.

(12) Xu, H.; Ye, H.; Osman, N. E.; Sadler, K.; Won, E. Y.; Chi, S. W.; Yoon, H. S. *Biochemistry* **2009,** *48,* 12159.

(13) Lin, J.; Chen, J.; Elenbaas, B.; Levine, A. J. *Genes Dev.* **1994,** *8,* 1235.

(14) Feng, H.; Jenkins, L. M.; Durell, S. R.; Hayashi, R.; Mazur, S. J.; Cherry, S.; Tropea, J. E.; Miller, M.; Wlodawer, A.; Appella, E.; Bai, Y. *Structure* **2009,** *17,* 202.

(15) Pazgier, M.; Liu, M.; Zou, G.; Yuan, W.; Li, C.; Li, J.; Monbo, J.; Zella, D.; Tarasov, S. G.; Lu, W. *Proc. Natl. Acad. Sci. U.S.A.* **2009,** *106,* 4665.

(16) Oltersdorf, T.; et al. *Nature* **2005,** *435,* 677.

(17) Kojima, K.; Konopleva, M.; McQueen, T.; O'Brien, S.; Plunkett, W.; Andreeff, M. *Blood* **2006,** *108,* 993.

(18) Vaseva, A. V.; Marchenko, N. D.; Moll, U. M. *Cell Cycle* **2009,** *8,* 1711.

(19) Kojima, K.; Konopleva, M.; Samudio, I. J.; Schober, W. D.; Bornmann, W. G.; Andreeff, M. *Cell Cycle* **2006,** *5,* 2778.